THE JOURNAL OF PHYSICAL CHEMISTRY Letters

Letter

pubs.acs.org/JPCL

Phonons Do Not Assist Carrier Multiplication in PbSe Quantum Dot Solids

Sybren ten Cate,[†] Yao Liu,[‡] Juleon M. Schins,[†] Matt Law,[‡] and Laurens D. A. Siebbeles*[,†]

[†]Optoelectronic Materials Section, Department of Chemical Engineering, Delft University of Technology, Julianalaan 136, 2628 BL Delft, The Netherlands

[‡]Department of Chemistry, University of California, Irvine, Irvine, California 92697, United States

ABSTRACT: Carrier multiplication (CM)—the Coulomb scattering whereby a sufficiently energetic charge excites a valence electron—is of interest for highly efficient quantum dot (QD) photovoltaics. Using time-resolved microwave conductivity experiments on 1,2-ethanedithiol-linked PbSe QD solids infilled with Al_2O_3 or Al_2O_3/ZnO by atomic layer deposition, we find that CM and hot-carrier cooling are temperature independent from 90–295 K and that spontaneous phonon emission limits the yield of charges resulting from the CM–cooling competition.

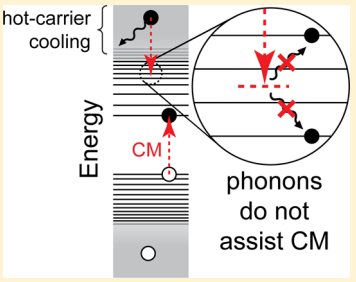

SECTION: Physical Processes in Nanomaterials and Nanostructures

Absorption of a sufficiently energetic photon by a material can lead to promotion of an electron from an occupied state to an initially empty state. In this way, an electron–hole pair is formed with an excess energy equal to the photon energy minus the lowest electronic excited state energy (band gap energy). The initially 'hot' electron and hole usually dissipate their excess energy ('cooling') as heat via interaction with nuclear lattice vibrations (phonons).[1] The hot electron and/or hole can also (partially) utilize their excess energy by exciting one or more valence electrons via Coulomb interaction. This phenomenon—carrier multiplication (CM; also called multiple exciton generation)—allows a single photon of sufficient energy to excite two or more electrons.[2−4] In recent years, CM has been demonstrated to occur in several types of colloidal semiconductor nanocrystals. Currently, CM in colloidal nanocrystals attracts a great deal of attention due to prospects for its utilization in cheap and highly efficient photovoltaics.[2−6]

In view of this, the dependence of the CM efficiency on various nanocrystal properties has received considerable interest. Nanocrystal composition (parent material[7−12] and architecture[13,14]) was found to affect the efficiency and threshold energy of CM due to variations in the effective masses of electron and hole and in the strength of the electron–phonon interaction.[15,16] Nanocrystal shape affects the CM efficiency, the latter being higher in elongated nanocrystals (nanorods) than in spherical nanocrystals (quantum dots, QDs).[17−20] In films of electronically coupled QDs (QD solids), the CM efficiency strongly varies with the nature of organic surface-passivating ligands and/or chemical treatment,[21] and with infilling of the interstitial space of the QD solid with inorganic matrices such as Al_2O_3 and ZnO.[22]

The effect of temperature on the CM efficiency has not yet been reported. The CM efficiency is determined through the competition of CM with hot-carrier cooling by phonon emission (Figure 1).[16,23] The latter process limits the time in

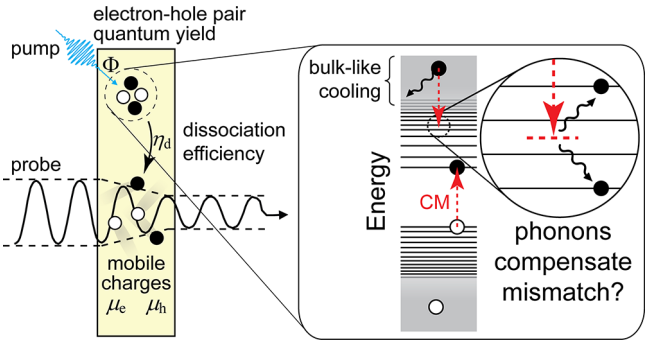

Figure 1. Illustration of the present study. Left: outline of the time-resolved microwave conductivity experiment. Right: sketch of the CM–cooling competition (determining the CM efficiency). Both CM and cooling may depend on temperature: CM because phonons may compensate energy mismatches, cooling because this occurs through phonon emission.

which CM can occur, thus reducing the CM efficiency. A hot single-exciton state has more decay channels to different multiexciton states when the temperature is higher and more phonons are available to assist CM by compensating for energy mismatches. The question arises to which extent the larger number of decay channels at higher temperatures enhances the CM rate. The cooling rate is also temperature dependent, since the amplitude of nuclear lattice vibrations, and thus the strength

Received: August 20, 2013
Accepted: September 16, 2013

   dx.doi.org/10.1021/jz401780w | J. Phys. Chem. Lett. 2013, 4, 3257−3262

of electron−phonon coupling, increases with temperature. How temperature affects the cooling rate, however, is not known *a priori*, since phonon absorption and stimulated phonon emission occur with different rates.

Here we report a study of the effect of temperature on CM (the process whereby a hot charge excites a valence electron), hot-carrier cooling, and the CM efficiency (related to the yield of electron−hole pairs generated per absorbed photon, and determined through the CM−cooling competition) in 1,2-ethanedithiol-capped PbSe (PbSe-EDT) QD solids infilled with Al_2O_3 or Al_2O_3/ZnO (1 nm of Al_2O_3 followed by 5 nm of ZnO) by atomic layer deposition. The PbSe QDs have a diameter of 6.3 nm, as determined via transmission electron microscopy. Synthesis of the PbSe QDs and preparation of the infilled QD solids are described in the Methods section. Infilling with Al_2O_3 or Al_2O_3/ZnO suppresses oxidative and photothermal degradation and passivates charge−trap states, leading to PbSe QD solids[24] in which CM occurs with an efficiency close to that of the QDs in solution.[22] The optical absorption spectra of the infilled PbSe-EDT QD solids (Figure 2) exhibit a band gap energy of E_g = 0.64 eV.

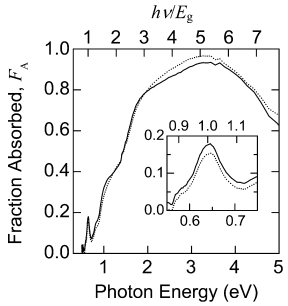

Figure 2. Optical absorption spectra of the Al_2O_3-infilled (solid line) and the Al_2O_3/ZnO-infilled (dotted line) PbSe-EDT QD solid at 295 K, showing the fraction of incident photons absorbed by the sample, F_A, as a function of photon energy in eV (bottom axis) or normalized to the band gap energy, $h\nu/E_g$ (top axis). Inset: magnified view of the first exciton peak.

The photoconductivity of the QD solids was determined from 90−295 K by time-resolved microwave conductivity (TRMC; see Methods),[25,26] similarly to our previous study at room temperature.[22] The samples were mounted in a rectangular microwave cavity (8.5 GHz resonance frequency) and excited with a 3 ns pump laser pulse of tunable wavelength. After a pump−probe delay time t, photogenerated mobile charges were probed by measuring the absorption of microwave power. The quantity derived from this is the sum of the quantum yields of mobile electrons and holes, $\phi_i(t)$, weighted by their mobilities, μ_i

$$\bar{\phi}(t) = \phi_e(t)\mu_e + \phi_h(t)\mu_h \quad (1)$$

where the transient quantum yield ϕ_e (or ϕ_h) equals the number of mobile electrons (or holes) per absorbed photon, and μ_e (or μ_h) the corresponding mobility.

According to our previous studies of these PbSe-EDT QD solids at room temperature, the threshold excitation energy for CM is $2.7E_g$.[22] In the present work, we study the effect of temperature on CM by comparing the photoconductivity at excitation energies of $1.9E_g$ (below the CM threshold, where CM does not occur) and $4.6E_g$ (above the CM threshold, where CM does occur).[22] Figure 3 shows $\bar{\phi}(t) = \phi_e(t)\mu_e + \phi_h(t)\mu_h$ obtained upon excitation at the above-mentioned photon energies at temperatures of 295 K (dotted curves) and 100 K (solid curves). An excitation fluence of 2×10^{-4} photons per QD was used, where higher-order recombination was found to be insignificant. The signal rises due to the generation of mobile charges on a time scale corresponding with the laser pulse duration. The signal reaches a maximum at $t = t_{max}$, determined by the balance between charge generation and charge decay during the laser pulse. The subsequent first-order decay kinetics of the signal is due to charge immobilization on traps and charge recombination and is independent of the excitation energy. This is expected because hot charges thermalize on a picosecond time scale, and the mobility of thermalized charges is independent of the initial energy on the longer time scale of Figure 3.[27,28] The signal has a higher initial value and decays faster at 295 K than at 100 K. The higher initial value is attributed to a thermally activated mobility and/or thermally activated (multi)exciton dissociation yield. The faster decay is attributed to a thermally activated mobility (a higher mobility decreases the charge lifetime by promoting trapping via faster diffusion) and/or thermally activated trapping. The apparent inconsistency of a thermally activated mobility with the temperature-independent mobility as found in similar samples using field-effect transistor measurements[29] can be explained by noting that traps states are filled in FET measurements, whereas trap states are not filled at the low carrier density presently used (ref 30 demonstrates this effect). At both temperatures, the signals at $h\nu = 4.6E_g$ are about 60% higher than at $h\nu = 1.9E_g$. This difference is attributed to a higher yield of charges produced via CM at the higher photon energy, in agreement with our earlier work.[22] The Al_2O_3/ZnO-infilled QD solid behaves similarly (data not shown).

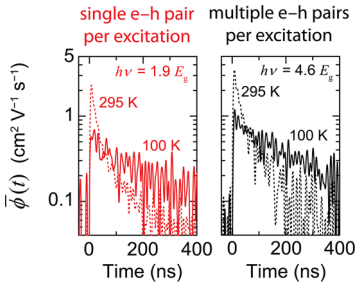

Figure 3. Effect of temperature on charge yield and decay for photon energies below (left panel; red) and above (right panel; black) the CM threshold energy in the Al_2O_3-infilled PbSe-EDT QD solid. Ordinate: sum of quantum yields of electrons and holes weighted by their mobility; i.e., $\bar{\phi}(t) = \phi_e(t)\mu_e + \phi_h(t)\mu_h$. The QD solid was excited at a fluence of 2×10^{-4} photons per QD where higher-order recombination is negligible.

Figure 4 shows Arrhenius plots of the maxima of the transient signals, $\bar{\phi}(t_{max}) = \phi_e(t_{max})\mu_e + \phi_h(t_{max})\mu_h$, obtained from data as in Figure 3, for excitation energies below (red) and above (black) the CM threshold. As the data form parallel straight lines in the Arrhenius graph, it follows that $\bar{\phi}(t_{max}) = f(h\nu)\exp[-E_A/(k_BT)]$, with f a scale factor and k_B the Boltzmann constant. A global fit (lines) yields E_A = (16.9 ± 0.3) meV (standard deviation, s.d.) for the Al_2O_3-infilled PbSe-EDT QD solid (panel A) and E_A = (15.3 ± 0.2) meV (s.d.) for the Al_2O_3/ZnO-infilled PbSe-EDT QD solid (panel B).[31] Note: E_A has no straightforward physical meaning, as outlined below. The identical temperature dependence of $\bar{\phi}(t_{max})$ in the absence and presence of CM immediately suggests that the

dx.doi.org/10.1021/jz401780w | J. Phys. Chem. Lett. 2013, 4, 3257−3262

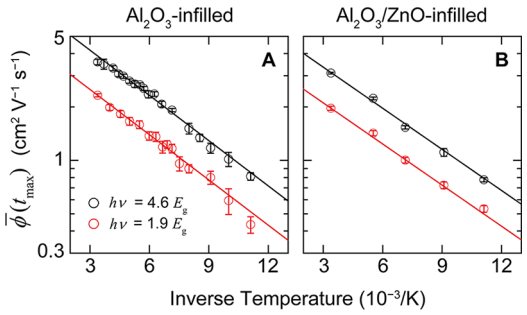

Figure 4. Arrhenius plots of $\bar{\phi}(t_{max})$ in the absence (red) and presence (black) of CM for (a) the Al_2O_3-infilled PbSe-EDT QD solid and (b) the Al_2O_3/ZnO-infilled PbSe-EDT QD solid. Error bars are standard deviations. Lines: Arrhenius fits show an identical activation energy above and below the CM threshold energy.

CM efficiency is temperature independent within the accuracy of our experiments. This is corroborated in the next paragraph.

The magnitude of the mobility-weighted sum of quantum yields of electrons and holes in Figures 3 and 4 is in general determined by: (1) the electron−hole (e−h) pair quantum yield, Φ, which is the number of e−h pairs generated per absorbed photon, and includes both e−h pairs bound as excitons and geminate pairs of free mobile charges, (2) the dissociation yield η_d, which is the efficiency with which an e−h pair yields free mobile charges, and (3) the survival fraction $s_i(t)$, which is the fraction of free mobile charges of species i that have not yet become trapped or recombined and are still present at time t after the pump laser pulse. Note, that according to our definition the e−h pair quantum yield Φ = 1 in the absence of CM because each absorbed photon generates one e−h pair, and Φ > 1 when CM occurs. Both Φ and η_d *can* depend on excitation energy $h\nu$ and on temperature T; i.e., $\Phi\eta_d \equiv \Phi(h\nu,T)\eta_d(h\nu,T)$. Using these definitions, the sum of the quantum yields of electrons and holes weighted by their mobility in Figure 4 is given by

$$\begin{aligned}\bar{\phi}(t_{max}) &= \Phi(h\nu,T)\eta_d(h\nu,T) \\ &\quad \times [s_e(t_{max},T)\mu_e(T) + s_h(t_{max},T)\mu_h(T)] \\ &\equiv f(h\nu)\exp[-E_A/(k_BT)]\end{aligned}$$

which can be rearranged to obtain

$$\frac{\Phi(h\nu,T)\eta_d(h\nu,T)}{f(h\nu)} = \frac{\exp\left(-\frac{E_A}{k_BT}\right)}{s_e(t_{max},T)\mu_e(T) + s_h(t_{max},T)\mu_h(T)} \quad (2)$$

The right-hand side of eq 2 is independent of the excitation energy, thus the left-hand side (LHS) of eq 2 must also be independent of the excitation energy. Therefore, the $h\nu$ dependence of the scale factor $f(h\nu)$ in the LHS denominator must completely cancel that of the product of the yields of e−h pair photogeneration and dissociation, i.e., $\Phi(h\nu,T)\eta_d(h\nu,T)$. This cancellation (by division) can occur only if the LHS numerator is proportional to $f(h\nu)$, i.e., if both yields are products of two mutually independent factors: one depending on photon energy, the other on temperature; i.e., $\Phi(h\nu,T) = \alpha(h\nu)\beta(T)$, and similarly for $\eta_d(h\nu,T)$.[32] At $h\nu = 1.9E_g$, it is energetically impossible for CM to occur (independent of temperature) so the e−h pair quantum yield is unity and temperature independent, i.e., $\Phi(1.9E_g,T) = 1$, and we may thus choose $\beta(T) = 1$. Hence, for both excitation energies, the e−h pair quantum yield is $\Phi(h\nu) = \alpha(h\nu)$, from which immediately follows that the CM efficiency is temperature independent.

Note: since the e−h pair quantum yield Φ is temperature independent, the Arrhenius behavior shown in Figure 4 must be due to a combination of (1) the dissociation yield η_d, (2) the mobilities μ_e and μ_h, and (3) the survival fractions s_e and s_h. Hence no straightforward physical meaning can presently be given for E_A.

Further insight into the factors that lead to the absence of an effect of temperature on the CM efficiency can be obtained as follows. A hot charge (electron or hole) can induce CM as long as its excess energy is larger than a certain threshold value (i.e., the QD band gap energy in the absence of momentum conservation restrictions). The CM efficiency is the outcome of the competition between CM and relaxation of hot charges to the threshold energy by phonon emission.[16,23] At each step of this relaxation process, the probability of CM is determined by the ratio of the CM rate to the sum of the CM- and phonon emission rate. In PbSe, electronic relaxation is predominantly due to polar interaction with longitudinal optical (LO) phonons of energy $\hbar\omega$ = 16.5 meV.[33,34] Hot charges in PbSe QDs behave to good approximation as in bulk,[4,35−37] and the rates of polar optical electron−phonon scattering are insensitive to effects of quantum confinement (become bulk-like) when the excess energy of the hot charge much exceeds the phonon energy,[38] as is presently the case. Thus, the cooling of hot charges in PbSe QDs occurs to good approximation as in bulk. In the bulk description for spherical parabolic bands, the change of the kinetic energy E of hot charges is[33]

$$\frac{dE}{dt} = C\left\{n(T)\,\sinh^{-1}\sqrt{\frac{E}{\hbar\omega}} - [n(T)+1]\,\sinh^{-1}\sqrt{\frac{E}{\hbar\omega}-1}\right\} \quad (3A)$$

with C a factor depending on the static and high-frequency dielectric constants, the phonon frequency and the charge velocity, and $\sinh^{-1}(z) \equiv \ln[z + (1+z^2)^{1/2}] \approx \ln(2z)$ for $z \gg 1$. Note: since C is strongly material dependent, material choice is very important in reducing the cooling rate and thereby improving the CM efficiency in QDs (and QD solids), as noted earlier.[16,18] The only temperature-dependent factor in eq 3A is the average phonon quantum number $n(T) = 1/(\exp[\hbar\omega/(k_BT)] - 1)$. The first term in eq 3A describes phonon absorption, and the second term represents stimulated- and spontaneous phonon emission. By collecting the temperature-dependent terms, eq 3A can be rewritten as

$$\frac{dE}{dt} = C\left[n(T)\left(\sinh^{-1}\sqrt{\frac{E}{\hbar\omega}} - \sinh^{-1}\sqrt{\frac{E}{\hbar\omega}-1}\right) - \sinh^{-1}\sqrt{\frac{E}{\hbar\omega}-1}\right] \quad (3B)$$

where the first term describes the difference of stimulated phonon absorption and emission, while the last term accounts for spontaneous phonon emission. In the present discussion, the kinetic energy E is at least equal to the excess energy required to undergo CM, i.e., $E \geq E_g$ = 0.64 eV. This value much exceeds the phonon energy, so that $E/(\hbar\omega) \geq 39$, and eq 3B becomes to excellent approximation (see Methods)

dx.doi.org/10.1021/jz401780w | J. Phys. Chem. Lett. 2013, 4, 3257−3262

$$\frac{dE}{dt} = \frac{C}{2}\left[n(T)\frac{\hbar\omega}{E} - \ln\left(\frac{4E}{\hbar\omega}\right)\right] \quad (3C)$$

The average number of LO phonons $n(T)$ is the only temperature-dependent factor and decreases from 1.09 at 295 K to 0.14 at 90 K. For $E \geq 0.64$ eV it is then found that the temperature-dependent term in eq 3C is more than 2 orders of magnitude smaller than the spontaneous phonon emission term (the second term). Hence, the cooling rate of hot electrons and holes is predominantly due to temperature-independent spontaneous phonon emission. Together with the observation of a temperature-independent CM efficiency, this implies that, like the cooling rate, the rate of CM itself does not vary with temperature. Hence, the availability of phonons insignificantly affects CM from 90−295 K. Apparently, the ability of phonons to compensate energy mismatches between a hot single-exciton state and different multiexciton states does not notably assist the CM rate.

In summary, we infer that phonons do not affect the rate of carrier multiplication itself. Furthermore, we have found that the CM efficiency is independent of temperature from 90 to 295 K. We argue that the CM efficiency is limited by fast cooling of hot charges, which we find to be dominated by the temperature-independent spontaneous emission of LO phonons.

METHODS

Chemicals. Chemicals were purchased from Aldrich and used as received.

QD Synthesis. PbSe QDs were synthesized by rapid precursor injection (15 mL of 1 M trioctylphosphine selenide containing 0.14 g diphenylphosphine) into a degassed and dried solution of lead oleate (1.09 g of PbO and 3.45 g of oleic acid in 13.5 g of 1-octadecene) at 180 °C. After 1 min of growth, the reaction was quenched, and the QDs then were three times precipitated/dispersed in ethanol/hexane and stored in an N_2-filled glovebox.

QD Solid Preparation. The QD solids were made by layer-by-layer dip coating. Quartz substrates, cleaned by sonication in acetone and isopropanol, were dipped consecutively in a 2 mg mL^{-1} suspension of QDs in hexane and a 1 mM solution of EDT in acetonitrile.

Atomic Layer Deposition Infilling. To prevent oxidative and photothermal degradation of the QD solids during TRMC experiments,[24] the interstitial spaces of the PbSe-EDT QD solids were infilled with Al_2O_3 or Al_2O_3/ZnO (1 nm of Al_2O_3 followed by 5 nm of ZnO) by low-temperature atomic layer deposition (ALD). The infilled QD solids were additionally overcoated with 20−30 nm of Al_2O_3 to further ensure their air stability. Amorphous Al_2O_3 was deposited by ALD of trimethylaluminum and water, and crystalline ZnO was deposited by ALD of diethylzinc and water. A substrate temperature of 75 °C, 20 ms pulse times, and 90−120 s purge times were used at a base pressure of $\sim 2 \times 10^{-4}$ bar.

Steady-State Optical Absorption. Absorption spectra were determined using the integrating sphere of a Perkin−Elmer Lambda 900 spectrometer. The band-gap energy of the QD solids, E_g, is taken as the energy at which the first absorption peak at room temperature is maximum. The QD band gap and the optical absorption cross section at the photoexcitation energies used in the experiments have negligible temperature dependence over 90−295 K.[39]

Time-Resolved Microwave Conductivity. The photoinduced change in microwave probe power P relates to the sum of quantum yields $\phi_i(t)$ for photogenerated electrons and holes weighted by their mobilities μ_i, as

$$\bar{\phi}(t) \equiv \phi_e(t)\mu_e + \phi_h(t)\mu_h = -\frac{A}{I_0 F_A}\left(\frac{P_{on}(t) - P_{off}}{P_{off}}\right)$$

with pump−probe delay time t, proportionality factor A,[22] incident laser pump fluence I_0, fraction of photons absorbed by the sample F_A (this quantity corrects for the wavelength-specific absorption of the sample), and subscript on (off) signifying the photoexcited (ground-state) film. The temperature of the films was regulated with ±0.1 K precision from 90−295 K using liquid nitrogen and power resistors. The excitation density was determined as the product of the reflection-reduced pump laser fluence and QD absorption cross section.[40] Note: this is the value of the excitation density at the interface of the sample where the pump light first enters. It is therefore a maximum value, and the excitation density will be lower in all other parts of the sample due to a Lambert−Beer absorption profile.

Transients were deconvolved with the microwave cavity response function $\exp(-t/\tau)$, with response time τ. The latter has the value $\tau = (\pi\Delta)^{-1}$, with Δ the full width at half-maximum of a Lorentzian reduction of the cavity reflection spectrum determined at five temperatures in the range of 90−295 K. The response time has a value of 15.9 ns (17.2 ns) at 295 K (90 K) and for intermediate temperatures T describes the second-order polynomial $\tau/\text{ns} = C_0 + C_1(T/\text{K}) + C_2(T/\text{K})^2$ with $C_0 = 16.37$, $C_1 = 1.37 \times 10^{-2}$, and $C_2 = -5.16 \times 10^{-5}$.

Absorption and Stimulated Emission of a Phonon by a Hot Charge. The energy rate of change for a hot charge of kinetic energy E (eq 3B) can be written as

$$\frac{dE}{dt} = C[X(T) - Y]$$

with

$$X(T) \equiv n(T)\left[\sinh^{-1}\sqrt{\frac{E}{\hbar\omega}} - \sinh^{-1}\sqrt{\frac{E}{\hbar\omega} - 1}\right],$$

$$Y \equiv \sinh^{-1}\sqrt{\frac{E}{\hbar\omega} - 1}$$

Defining $x \equiv E/(\hbar\omega)$, we can write

$$X(T) = n(T)[\sinh^{-1}\sqrt{x} - \sinh^{-1}\sqrt{x-1}] \quad (A)$$

Since in the present work $x \gg 1$, because the charge energy much exceeds the phonon energy, the first of the two square roots can be expanded via the binomial series

$$\sqrt{x-1} = \sqrt{x}\sqrt{1 - \frac{1}{x}} = \sqrt{x} - \frac{1}{2\sqrt{x}} + \ldots$$

$$\equiv \sqrt{x} + \Delta \Leftrightarrow \Delta \equiv \sqrt{x-1} - \sqrt{x}$$

Substituting this expression into eq A and multiplying by Δ/Δ yields

$$X(T) = -n(T)\Delta\left[\frac{\sinh^{-1}(\sqrt{x} + \Delta) - \sinh^{-1}\sqrt{x}}{\Delta}\right]$$

$$= -n(T)\Delta\frac{d\sinh^{-1}\sqrt{x}}{d\sqrt{x}} = -n(T)\frac{\Delta}{\sqrt{x+1}},$$

$$\text{for } \Delta \to 0$$

dx.doi.org/10.1021/jz401780w | J. Phys. Chem. Lett. 2013, 4, 3257−3262

Because in the present work $\Delta \to 0$, we may write (substituting the expression for Δ)

$$X(T) \approx n(T)\left(\frac{\sqrt{x} - \sqrt{x-1}}{\sqrt{x+1}}\right)$$

Expanding the square roots via the binomial series, neglecting terms of second order and higher, and substituting the expression for x gives

$$X(T) \approx n(T)\frac{\hbar\omega}{2E + \hbar\omega} \approx n(T)\frac{\hbar\omega}{2E} \quad \text{(B)}$$

Equation B becomes exactly identical to equation A in the limit when $E/(\hbar\omega)$ tends to infinity, and is very nearly identical for $E \gg \hbar\omega$. At present, $E/(\hbar\omega) \geq 39$ and equation B is an excellent approximation to eq A.

The expression for Y may be simplified using the definition $\sinh^{-1}(z) \equiv \ln[z + (1 + z^2)^{1/2}]$ (which well approximates $\ln(2z)$ for $z \gg 1$), and by noting that $E/(\hbar\omega) \gg 1$ in the present work, to yield

$$Y \approx \ln\left(2\sqrt{\frac{E}{\hbar\omega}}\right) = \frac{1}{2}\ln\left(\frac{4E}{\hbar\omega}\right)$$

Thus for hot charges, eq 3B simplifies to

$$\frac{dE}{dt} = \frac{C}{2}\left[n(T)\frac{\hbar\omega}{E} - \ln\left(\frac{4E}{\hbar\omega}\right)\right]$$

AUTHOR INFORMATION

Corresponding Author

*E-mail: l.d.a.siebbeles@tudelft.nl.

Author Contributions

S.t.C. performed the experiments and analysis, and wrote the manuscript. Y.L. synthesized the QDs, prepared the QD solids, and performed the ALD infilling. J.M.S. advised on the experimental work. M.L. and L.D.A.S. designed and supervised the project and edited the manuscript.

Notes

The authors declare no competing financial interest.

ACKNOWLEDGMENTS

This work is part of the Joint Solar Programme (JSP) of Hyet Solar and the Stichting voor Fundamenteel Onderzoek der Materie (FOM), which is part of the Nederlandse Organisatie voor Wetenschappelijk Onderzoek (NWO). Y.L. and M.L. acknowledge financial support by the Center for Advanced Solar Photophysics (CASP), an Energy Frontier Research Center funded by the U.S. Department of Energy (DOE), Office of Science, Office of Basic Energy Sciences (BES).

REFERENCES

(1) Kambhampati, P. Unraveling the Structure and Dynamics of Excitons in Semiconductor Quantum Dots. *Acc. Chem. Res.* **2011**, *44*, 1−13.

(2) Beard, M. C.; Luther, J. M.; Semonin, O. E.; Nozik, A. J. Third Generation Photovoltaics based on Multiple Exciton Generation in Quantum Confined Semiconductors. *Acc. Chem. Res.* **2013**, *46*, 1252−1260.

(3) Beard, M. C. Multiple Exciton Generation in Semiconductor Quantum Dots. *J. Phys. Chem. Lett.* **2011**, *2*, 1282−1288.

(4) Nair, G.; Chang, L. Y.; Geyer, S. M.; Bawendi, M. G. Perspective on the Prospects of a Carrier Multiplication Nanocrystal Solar Cell. *Nano Lett.* **2011**, *11*, 2145−2151.

(5) Sargent, E. H. Colloidal Quantum Dot Solar Cells. *Nat. Photonics* **2012**, *6*, 133−135.

(6) Semonin, O. E.; Luther, J. M.; Choi, S.; Chen, H.-Y.; Gao, J.; Nozik, A. J.; Beard, M. C. Peak External Photocurrent Quantum Efficiency Exceeding 100% via MEG in a Quantum Dot Solar Cell. *Science* **2011**, *334*, 1530−1533.

(7) Trinh, M. T.; Limpens, R.; de Boer, W. D. A. M.; Schins, J. M.; Siebbeles, L. D. A.; Gregorkiewicz, T. Direct Generation of Multiple Excitons in Adjacent Silicon Nanocrystals Revealed by Induced Absorption. *Nat. Photonics* **2012**, *6*, 316−321.

(8) Timmerman, D.; Valenta, J.; Dohnalova, K.; de Boer, W. D. A. M.; Gregorkiewicz, T. Step-Like Enhancement of Luminescence Quantum Yield of Silicon Nanocrystals. *Nat. Nanotechnol.* **2011**, *6*, 710−713.

(9) Nozik, A. J.; Beard, M. C.; Luther, J. M.; Law, M.; Ellingson, R. J.; Johnson, J. C. Semiconductor Quantum Dots and Quantum Dot Arrays and Applications of Multiple Exciton Generation to Third-Generation Photovoltaic Solar Cells. *Chem. Rev.* **2010**, *110*, 6873−6890.

(10) Stubbs, S. K.; Hardman, S. J. O.; Graham, D. M.; Spencer, B. F.; Flavell, W. R.; Glarvey, P.; Masala, O.; Pickett, N. L.; Binks, D. J. Efficient Carrier Multiplication in InP Nanoparticles. *Phys. Rev. B* **2010**, *81*, 081303.

(11) Beard, M. C.; Knutsen, K. P.; Yu, P. R.; Luther, J. M.; Song, Q.; Metzger, W. K.; Ellingson, R. J.; Nozik, A. J. Multiple Exciton Generation in Colloidal Silicon Nanocrystals. *Nano Lett.* **2007**, *7*, 2506−2512.

(12) Nair, G.; Bawendi, M. G. Carrier Multiplication Yields of CdSe and CdTe Nanocrystals by Transient Photoluminescence Spectroscopy. *Phys. Rev. B* **2007**, *76*, 081304.

(13) Trinh, M. T.; Polak, L.; Schins, J. M.; Houtepen, A. J.; Vaxenburg, R.; Maikov, G. I.; Grinbom, G.; Midgett, A. G.; Luther, J. M.; Beard, M. C.; et al. Anomalous Independence of Multiple Exciton Generation on Different Group IV−VI Quantum Dot Architectures. *Nano Lett.* **2011**, *11*, 1623−1629.

(14) Gachet, D.; Avidan, A.; Pinkas, I.; Oron, D. An Upper Bound to Carrier Multiplication Efficiency in Type II Colloidal Quantum Dots. *Nano Lett.* **2010**, *10*, 164−170.

(15) Zohar, G.; Baer, R.; Rabani, E. Multiexciton Generation in IV−VI Nanocrystals: The Role of Carrier Effective Mass, Band Mixing, and Phonon Emission. *J. Phys. Chem. Lett.* **2013**, *4*, 317−322.

(16) Stewart, J. T.; Padilha, L. A.; Qazilbash, M. M.; Pietryga, J. M.; Midgett, A. G.; Luther, J. M.; Beard, M. C.; Nozik, A. J.; Klimov, V. I. Comparison of Carrier Multiplication Yields in PbS and PbSe Nanocrystals: The Role of Competing Energy-Loss Processes. *Nano Lett.* **2011**, *12*, 622−628.

(17) Cunningham, P. D.; Boercker, J. E.; Foos, E. E.; Lumb, M. P.; Smith, A. R.; Tischler, J. G.; Melinger, J. S. Correction to Enhanced Multiple Exciton Generation in Quasi-One-Dimensional Semiconductors. *Nano Lett.* **2013**, *13*, 3003.

(18) Padilha, L. A.; Stewart, J. T.; Sandberg, R. L.; Bae, W. K.; Koh, W.-K.; Pietryga, J. M.; Klimov, V. I. Carrier Multiplication in Semiconductor Nanocrystals: Influence of Size, Shape, and Composition. *Acc. Chem. Res.* **2013**, *46*, 1261−1269.

(19) Padilha, L. A.; Stewart, J. T.; Sandberg, R. L.; Bae, W. K.; Koh, W. K.; Pietryga, J. M.; Klimov, V. I. Aspect Ratio Dependence of Auger Recombination and Carrier Multiplication in PbSe Nanorods. *Nano Lett.* **2013**, *13*, 1092−1099.

(20) Cunningham, P. D.; Boercker, J. E.; Foos, E. E.; Lumb, M. P.; Smith, A. R.; Tischler, J. G.; Melinger, J. S. Enhanced Multiple Exciton Generation in Quasi-One-Dimensional Semiconductors. *Nano Lett.* **2011**, *11*, 3476−3481.

(21) Beard, M. C.; Midgett, A. G.; Law, M.; Semonin, O. E.; Ellingson, R. J.; Nozik, A. J. Variations in the Quantum Efficiency of Multiple Exciton Generation for a Series of Chemically Treated PbSe Nanocrystal Films. *Nano Lett.* **2009**, *9*, 836−845.

(22) ten Cate, S.; Liu, Y.; Suchand Sandeep, C. S.; Kinge, S.; Houtepen, A. J.; Savenije, T. J.; Schins, J. M.; Law, M.; Siebbeles, L. D. A. Activating Carrier Multiplication in PbSe Quantum Dot Solids by

Infilling with Atomic Layer Deposition. *J. Phys. Chem. Lett.* **2013**, *4*, 1766−1770.
(23) Beard, M. C.; Midgett, A. G.; Hanna, M. C.; Luther, J. M.; Hughes, B. K.; Nozik, A. J. Comparing Multiple Exciton Generation in Quantum Dots To Impact Ionization in Bulk Semiconductors: Implications for Enhancement of Solar Energy Conversion. *Nano Lett.* **2010**, *10*, 3019−3027.
(24) Liu, Y.; Gibbs, M.; Perkins, C.; Tolentino, J.; Zarghami, M.; Bustamante, J.; Law, M. Robust, Functional Nanocrystal Solids by Infilling with Atomic Layer Deposition. *Nano Lett.* **2011**, *11*, 5349−5404.
(25) Kroeze, J. E.; Savenije, T. J.; Vermeulen, M. J. W.; Warman, J. M. Contactless Determination of the Photoconductivity Action Spectrum, Exciton Diffusion Length, and Charge Separation Efficiency in Polythiophene-Sensitized TiO_2 Bilayers. *J. Phys. Chem. B* **2003**, *107*, 7696−7705.
(26) De Haas, M. P.; Warman, J. M. Photon-Induced Molecular Charge Separation Studied by Nanosecond Time-Resolved Microwave Conductivity. *Chem. Phys.* **1982**, *73*, 35−53.
(27) Miaja-Avila, L.; Tritsch, J. R.; Wolcott, A.; Chan, W. L.; Nelson, C. A.; Zhu, X. Y. Direct Mapping of Hot-Electron Relaxation and Multiplication Dynamics in PbSe Quantum Dots. *Nano Lett.* **2012**, *12*, 1588−1591.
(28) Gao, Y. N.; Talgorn, E.; Aerts, M.; Trinh, M. T.; Schins, J. M.; Houtepen, A. J.; Siebbeles, L. D. A. Enhanced Hot-Carrier Cooling and Ultrafast Spectral Diffusion in Strongly Coupled PbSe Quantum-Dot Solids. *Nano Lett.* **2011**, *11*, 5471−5476.
(29) Liu, Y.; Tolentino, J.; Gibbs, M.; Ihly, R.; Perkins, C. L.; Liu, Y.; Crawford, N.; Hemminger, J. C.; Law, M. PbSe Quantum Dot Field-Effect Transistors with Air-Stable Electron Mobilities above 7 $cm^2\ V^{-1}\ s^{-1}$. *Nano Lett.* **2013**, *13*, 1578−1587.
(30) Talgorn, E.; Gao, Y.; Aerts, M.; Kunneman, L. T.; Schins, J. M.; Savenije, T. J.; Van Huis, M. A.; Van der Zant, H. S. J.; Houtepen, A. J.; Siebbeles, L. D. A. Unity Quantum Yield of Photogenerated Charges and Band-Like Transport in Quantum-Dot Solids. *Nat. Nanotechnol.* **2011**, *6*, 733−739.
(31) Note: E_A is presently determined from the end-of-pulse signal (at $t = t_{max}$). Its value would be higher when determined at $(t = 0)$ due to the temperature-activated charge decay within the laser pulse.
(32) Reasonably, Φ and η_d are not inversely proportional to each other since they correspond to the physically distinct processes of generation and dissociation.
(33) Ridley, B. K. Lattice Scattering. In *Quantum Processes in Semiconductors*, 4th ed.; Clarendon Press: Oxford, 1999.
(34) Collaboration: Authors and editors of the volumes III/17E-17F-41C: *Lead Selenide (PbSe) Phonon Frequencies, Sound Velocities*; Madelung, O., Rössler, U., Schulz, M., Eds.; SpringerMaterials - The Landolt-Börnstein Database; Vol. *41C*. DOI: 10.1007/10681727_892.
(35) Cho, B.; Peters, W. K.; Hill, R. J.; Courtney, T. L.; Jonas, D. M. Bulklike Hot Carrier Dynamics in Lead Sulfide Quantum Dots. *Nano Lett.* **2010**, *10*, 2498−2505.
(36) Delerue, C.; Allan, G.; Pijpers, J. J. H.; Bonn, M. Carrier Multiplication in Bulk and Nanocrystalline Semiconductors: Mechanism, Efficiency, and Interest for Solar Cells. *Phys. Rev. B* **2010**, *81*, 125306.
(37) Moreels, I. *Colloidal Semiconductor Nanocrystals: From Synthesis to Photonic Applications*; Ghent University, Ghent, Belgium, 2009; 131−132.
(38) Riddoch, F. A.; Ridley, B. K. Phonon Scattering of Electrons in Quasi-One-Dimensional and Quasi-Two-Dimensional Quantum Wells. *Surf. Sci.* **1984**, *142*, 260−265.
(39) Olkhovets, A.; Hsu, R. C.; Lipovskii, A.; Wise, F. W. Size-Dependent Temperature Variation of the Energy Gap in Lead-Salt Quantum Dots. *Phys. Rev. Lett.* **1998**, *81*, 3539−3542.
(40) Moreels, I.; Lambert, K.; De Muynck, D.; Vanhaecke, F.; Poelman, D.; Martins, J. C.; Allan, G.; Hens, Z. Composition and Size-Dependent Extinction Coefficient of Colloidal PbSe Quantum Dots. *Chem. Mater.* **2007**, *19*, 6101−6106.